# Biological Chemistry ‘Just Accepted’ Papers

**Biological Chemistry ‘Just Accepted’ Papers** are papers published online, in advance of appearing in the print journal. They have been peer-reviewed, accepted and are online published in manuscript form, but have not been copy edited, typeset, or proofread. Copy editing may lead to small differences between the Just Accepted version and the final version. There may also be differences in the quality of the graphics. When papers do appear in print, they will be removed from this feature and grouped with other papers in an issue.

**Biol Chem ‘Just Accepted’ Papers** are citable; the online publication date is indicated on the Table of Contents page, and the article’s Digital Object Identifier (DOI), a unique identifier for intellectual property in the digital environment (e.g., 10.1515/hsz-2011-xxxx), is shown at the top margin of the title page. Once an article is published as **Biol Chem ‘Just Accepted’ Paper** (and before it is published in its final form), it should be cited in other articles by indicating author list, title and DOI.

After a paper is published in **Biol Chem ‘Just Accepted’ Paper** form, it proceeds through the normal production process, which includes copy editing, typesetting and proofreading. The edited paper is then published in its final form in a regular print and online issue of **Biol Chem.** At this time, the **Biol Chem ‘Just Accepted’ Paper** version is replaced on the journal Web site by the final version of the paper with the same DOI as the **Biol Chem ‘Just Accepted’ Paper version.**

## Disclaimer

**Biol Chem ‘Just Accepted’ Papers** have undergone the complete peer-review process. However, none of the additional editorial preparation, which includes copy editing, typesetting and proofreading, has been performed. Therefore, there may be errors in articles published as **Biol Chem ‘Just Accepted’ Papers** that will be corrected in the final print and online version of the Journal. Any use of these articles is subject to the explicit understanding that the papers have not yet gone through the full quality control process prior to advanced publication.

*Biological Chemistry* **'Just Accepted' paper**
**ISSN (online) 1437-4315**
**DOI: 10.1515/hsz-2017-0309**

**Research Article**

# *In vitro* reconstitution and biochemical characterization of human phospholipid scramblase 3: phospholipid specificity and metal ion binding studies

Santosh Kumar Palanirajan, Ulaganathan Sivagnanam, Sowmiya Murugan and Sathyanarayana N. Gummadi*

Applied and Industrial Microbiology Laboratory, Department of Biotechnology, Bhupat and Jyoti Mehta School of Biosciences, Indian Institute of Technology Madras, Chennai 600 036, India

*Corresponding author

e-mail: gummadi@iitm.ac.in

## Abstract

Human phospholipid scramblase 3 (hPLSCR3) is a single pass transmembrane protein that plays a vital role in fat metabolism, mitochondrial function, structure, maintenance and apoptosis. The mechanism of action of scramblases remains still unknown and the role of scramblases in phospholipid translocation is heavily debated. hPLSCR3 is the only member of scramblase family localized to mitochondria and is involved in cardiolipin translocation at the mitochondrial membrane. Direct biochemical evidence of phospholipid translocation by hPLSCR3 is yet to be reported. Functional assay in synthetic proteoliposomes upon $Ca^{2+}$ and $Mg^{2+}$ revealed that, apart from cardiolipin, recombinant hPLSCR3 translocates aminophospholipids such as NBD-PE and NBD-PS but not neutral phospholipids. Point mutation in hPLSCR3 (F258V) resulted in decreased $Ca^{2+}$ binding affinity. Functional assay with F258V-hPLSCR3 led to ~50% loss in scramblase activity in the presence of $Ca^{2+}$ and $Mg^{2+}$. Metal ion induced conformational changes were monitored by intrinsic tryptophan fluorescence, circular dichroism, surface hydrophobicity changes and aggregation studies. Our results revealed that $Ca^{2+}$ and $Mg^{2+}$ bind to hPLSCR3 and trigger conformational changes mediated by aggregation. In summary, we suggest that the metal ion induced conformational change and the aggregation of the protein is essential for the phospholipid translocation by hPLSCR3.


**Keywords:** aggregation; $Ca^{2+}$ binding; hPLSCR3; lipid translocation; transmembrane protein.

# Introduction

Phospholipid scramblases (PLSCRs) are a group of type II single pass transmembrane proteins involved in the ATP-independent and $Ca^{2+}$ dependent bidirectional translocation of phospholipids (PL) between the two leaflets of the lipid bilayer (Bevers *et al.*, 1998). PLSCRs are a family of five homologous proteins conserved from *C. elegans* to humans (Sahu *et al.*, 2007). In humans, these five homologous proteins are termed as hPLSCR1-5 of which hPLSCR3 is located at chromosome 3 and the rest of the members are clustered at chromosome 17 (Wiedmer *et al.*, 2000). Multiple sequence alignment of hPLSCRs from different species revealed the presence of several conserved regions which include, a $Ca^{2+}$-binding EF-hand like motif (Zhou *et al.*, 1998, Bassé *et al.*, 1996), DNA binding domain (Zhou *et al.*, 2005), nuclear localization signal (Lott *et al.*, 2011), palmitoylation motif (Zhao *et al.*, 1998b), a single-pass transmembrane domain (Francis *et al.*, 2013) and the recently identified cholesterol binding domain (Posada *et al.*, 2014). Though primarily a membrane protein, hPLSCRs are known to be localized to cytoplasm and nucleus apart from plasma membrane. hPLSCR1 and hPLSCR4 were known to be localized to plasma membrane, and nucleus whereas hPLSCR2 showed exclusive nuclear localization. hPLSCR3 is the only member of scramblase family that localizes to mitochondria.

hPLSCR3 is the most extensively studied member of scramblase family apart from hPLSCR1 and was shown to have crucial roles in mitochondrial morphology, respiratory function, fat metabolism and apoptosis. hPLSCR3 mediates the translocation of cardiolipin (CL) from the inner membrane to outer membrane of mitochondria. Protein kinase C-δ (PKC-δ) interacts with hPLSCR3 and phosphorylates at $Thr^{21}$ thereby activating hPLSCR3. Activated hPLSCR3 in the presence of high concentration of $Ca^{2+}$ triggers CL exposure to the outer mitochondrial membrane. CL in the outer membrane recruits t-BID which in-turn positively regulates hPLSCR3 for further CL translocation eventually leading to release of cytochrome C, a hallmark of apoptosis (Liu *et al.*, 2008, Sivagnanam *et al.*, 2017).

Cells expressing hPLSCR3 showed enhanced *de novo* biosynthesis and decreased resynthesis of CL in HeLa cells. Wild-type PLSCR3 (wt-hPLSCR3) showed normal mitochondrial morphology and enhanced levels of mitochondrial mass, apoptotic sensitivity and CL translocation. A report by Zhou *et al.*,, revealed that the mutations in calcium binding motif of hPLSCR1 at positions 1, 3, 5, 7, 9 and 12 impaired scrambling activity with the mutations at D and F ($3^{rd}$ and $9^{th}$ position) rendered the protein completely inactive. Based on this study, a

point mutant was generated with mutation (F258V) in the calcium binding motif ($9^{th}$ position) of hPLSCR3. Stable transfectants of F258V-hPLSCR3 in HEK293 cells showed reduced proliferative capacity, decreased mitochondrial mass and transmembrane potential, reduced CL content, poor respiration and lower ATP levels compared to wt-hPLSCR3 (Liu *et al.*, 2008). Further results revealed that F258V-hPLSCR3 showed abnormal mitochondrial metabolism, altered structure, weakened CL translocation and reduced sensitivity to UV and tBid-induced apoptosis.

Although the role of hPLSCR3 in CL translocation was reported in vivo, several key questions still exist: (i) How does hPLSCR3 translocates PL *in vitro*? (ii) How does $Ca^{2+}$ regulate hPLSCR3 activity and what is the binding affinity of $Ca^{2+}$ to hPLSCR3? (iii) Does hPLSCR3 exhibit PL head group specificity in membrane translocation? (iv) What is the effect of F258V mutation in in vitro activity of hPLSCR3? To address these questions, we recombinantly cloned and overexpressed wt-hPLSCR3 and F258V-hPLSCR3 in bacterial expression system and purified using the protocol optimized for scramblases. We have demonstrated the scrambling activity of hPLSCR3 and the mutant F258V-hPLSCR3 in the presence of $Ca^{2+}$ and $Mg^{2+}$ in synthetic proteoliposomes with different phospholipids. The binding affinity and the conformational changes upon binding to $Ca^{2+}$ and $Mg^{2+}$ were determined by spectroscopic techniques.

# Results

## Overexpression and purification of the recombinant wt-hPLSCR3 and F258V-hPLSCR3

hPLSCR3 ORF was sub-cloned into pET-28 a(+) vector and overexpressed in *Escherichia coli* Rosetta (DE3) as 6×His-hPLSCR3. It was observed that the overexpressed hPLSCR3 was predominantly distributed in the insoluble fraction implying the occurrence of proteins in inclusion bodies (IBs) (Figure 1A). The SDS PAGE analysis revealed that the recombinant protein showed a molecular mass of ~ 34 kDa which corroborates with previous reports (Liu *et al.*, 2008). N-lauroyl sarcosine (NLS), an anionic detergent, was used to solubilise IBs overnight (Francis *et al.*, 2012a). NLS treatment resulted in recovery of ~40-50% of target protein from the IBs. The supernatant fraction after NLS treatment was dialysed against buffer A containing 0.025% Brij-35, a mild non-ionic detergent that acts as a counter

detergent for enhancing the stability of soluble hPLSCR3 (Francis and Gummadi, 2012). The dialysed supernatant was then loaded on to a $Ni^{2+}$-NTA column and the bound protein was eluted with 250 mM imidazole. The final yield of 95% pure protein was ~1 mg/g cell mass (Figure 1B). The purified recombinant hPLSCR3 was further confirmed by Western blotting (Figure 1C). The molecular weight and the oligomeric state of the purified protein is established by size exclusion chromatography. From the elution volume (Ve) it was observed that the purified protein exists as monomer and the molecular weight is calculated to be 34.3 kDa (from standard plot) which corresponds to the theoretical molecular weight (Figure 1D). A multiple sequence alignment revealed that the 12 amino acids constituting the $Ca^{2+}$ binding motif in scramblase family of proteins was highly conserved across species (Figure 1E). The amino acids at position 1, 3, 5, 9, 10 and 12 are highly conserved with positions 1,3 and 12 having charged amino acids and 5, 9, 10 with hydrophobic amino acids. The conserved amino acids have a dominant role in the $Ca^{2+}$ binding ability of the protein and its biological function. Based on the previous reports, a point mutation, F258V resulted in diminished functional activity of hPLSCR3. F258V- hPLSCR3 was generated by site directed mutagenesis, overexpressed and purified as 6×His-F258V-hPLSCR3 in line with the above-mentioned method and a final yield of about 1 mg/g cells was used for subsequent studies.

## Biochemical reconstitution and functional scramblase assay

To determine whether hPLSCR3 is involved in scrambling of PLs across the bilayer in the presence of elevated levels of calcium, we reconstituted wt-hPLSCR3 and F258V-hPLSCR3 in to synthetic proteoliposomes and scramblase activity was initiated by the addition of $Ca^{2+}$ or $Mg^{2+}$ (Figure 2). A basic schematic of the scramblase assay was given in Figure S1. wt-hPLSCR3 exhibited a scrambling activity of about 10% against outside labelled NBD-PE vesicles selectively (Figure 2D) when compared to NBD-PS, NBD-PG and NBD-PC (Figure 2A-C). Scramblase activity performed in the presence of $Mg^{2+}$ showed transbilayer movement of PLs similar to that of $Ca^{2+}$ (Figure 2A-2D). The point mutant F258V-hPLSCR3 showed ~40% to ~50% decrease in scrambling activity compared to wt-hPLSCR3 for NBD-PE (Figure 2H) and negligible activity for NBD-PS, NBD-PG, and NBD-PC (Figure 2E-G). Statistical analysis for assay with outside labelled proteoliposomes revealed that wt-hPLSCR3 (Figure 3A) and F258V-hPLSCR3 (Figure 3B) showed significant translocation of NBD-PE when compared to other labelled phospholipids. Since, hPLSCR1 was shown to scramblase PLs, scramblase activity was also measured for inside lablelled

vesicles. Assay with inside labelled proteoliposomes revealed that wt-hPLSCR3 sequestered ~11% and ~8% NBD-PE outside in the presence of $Ca^{2+}$ and $Mg^{2+}$ respectively. F258V-hPLSCR3 mutant showed ~40% and 10% loss of activity in the presence of $Ca^{2+}$ and $Mg^{2+}$ respectively (Figure 3C).

## Intrinsic tryptophan fluorescence

The intrinsic tryptophan fluorescence was measured to estimate the affinity of metal ions to hPLSCR3. Curve fitting was done for the fraction of ligand sites occupied $[(F_0 - F)/(F_0 - F_{sat})]$ vs. ligand concentration using the one-site binding nonlinear regression analysis, where $F_0$ is the maximum fluorescence in the absence of a ligand, $F_{sat}$ is the maximum fluorescence at saturated ligand concentration, and F is the fluorescence at a particular ligand concentration. Dissociation constants ($K_d$) were determined by Scatchard plot using nonlinear curve fitting (Prism 5.0 GraphPad Prism Inc., San Diego, USA). wt-hPLSCR3 showed similar binding affinities for $Ca^{2+}$ and $Mg^{2+}$ with $K_d$ values of 23.31 mM ± 1.90 mM and 20.98 mM ± 1.55 mM respectively (Figure 4A, 4B). F258V-hPLSCR3 showed ~ 50% decrease in affinity for $Ca^{2+}$ and $Mg^{2+}$ compared to wt-hPLSCR3 with $K_d$ values of 54.85 ± 4.12 mM and 77.76 ± 9.51 mM respectively (Figure 4C, 4D). The marked decrease in binding affinity for F258V-hPLSCR3 compared to wt-hPLSCR3 revealed that the predicted $Ca^{2+}$ -binding motif is indeed the $Ca^{2+}$ binding site in the protein.

## Far-UV CD spectroscopy

Far-UV CD spectroscopy is done to further confirm the metal ion induced structural changes with hPLSCR3. It was observed that the apo form of the hPLSCR3 was characterized by two distinct minima at 208 and 220 nm, characteristic of a typical α -helix conformational elements (Figure 5A and B) in a protein. In the presence of $Ca^{2+}$ and $Mg^{2+}$, spectral changes were observed in the CD spectra of wt-hPLSCR3 with the intensities of the distinct minima decreasing (Figure 5A and B). F258V-hPLSCR3 showed a relatively small increase in β sheet like conformational elements with distinct minima at 215 nm (Figure 5C and D). These results indicate that hPLSCR3 undergoes similar conformational changes in the protein upon addition of $Ca^{2+}$ and $Mg^{2+}$. These conformational changes could be vital for proper folding and functioning of the protein.

## Probing conformational (surface hydrophobicity) changes by 8-anilino-1-naphthalenesulfonic acid fluorescence

8-Anilino-1-naphthalenesulfonic acid (ANS) is fluorescent only in a nonpolar environment, and its fluorescence is quenched in the presence of a polar environment (Daniel and Weber, 1966). Studies on the surface hydrophobicity changes provide valuable information on the conformation of the protein upon binding to protein complexes, metal ions, substrates etc (Cardamone and Puri, 1992, Alizadeh-Pasdar and Li-Chan, 2000). ANS was used to study metal ion-induced changes in the surface hydrophobicity of hPLSCR3. In Figure 6, trace a represents the fluorescence emission of the ANS protein complex in the absence of metal ions. In the presence of metal ions, enhanced ANS fluorescence was observed (Figure 6, traces b, c, and d). Binding of $Ca^{2+}$ and $Mg^{2+}$ induce local conformational changes altering the structure of hPLSCR3 leading to the exposure of hydrophobic residues for which binds to ANS resulting in an increase in fluorescence emission. F258V-hPLSCR3 showed similar ANS binding pattern as that of wt-hPLSCR3. Results reveal that even with reduced binding affinity, F258V-hPLSCR3 could still exhibit conformational change upon metal binding and expose hydrophobic residues to the surface. Exposure of hydrophobic residues to the surface could trigger interactions with other proteins or could induce oligomerization/aggregation of the protein.

## Aggregation studies

Increase in the absorption spectra at 360 nm denotes protein aggregation (Liu *et al.*, 2003). Since, metal ion induces exposure of hydrophobic patches to the surface that could lead to oligomerization of hPLSCR3, aggregation studies were performed. An increase in the absorbance at 360 nm upon addition of metal ions, with respect to time denotes aggregation of the protein. wt-hPLSCR3 and F258V-hPLSCR3, in the absence of metal ions, showed very low absorbance. When $Ca^{2+}$ was added, the increase in absorbance was observed for both the proteins upon treatment with increasing concentrations of $Ca^{2+}$ and was saturated at 30 mM (Figure 7A and B). $Mg^{2+}$ induced aggregation was significantly less compared to $Ca^{2+}$ in wt-hPSLCR3 and F258V-hPLSCR3 (Figure 7A and B). The increase in absorbance after a time period of 1200 s was monitored for different concentrations of metal ions and was observed that the aggregation of F258V-hPLSCR3 is similar to that of wt-hPLSCR3 at 1200 s. These results suggest that the aggregation potential of the protein remains unaffected by the mutation in the calcium-binding motif.

# Discussion

This is the first report on the *in vitro* biochemical characterization of recombinant hPLSCR3. hPLSCR3 has gained interest in the past decade due to its central role in mitochondrial processes and the only member of scramblase family localized to mitochondria (Liu *et al.*, 2003). hPLSCR3 is involved in mitochondrial membrane biogenesis, mitochondrial apoptosis (intrinsic pathway) and translocates CL upon $Ca^{2+}$ activation (Liu *et al.*, 2003, Van *et al.*, 2007, He *et al.*, 2007). Previous reports suggested that mutation of $Phe^{258}$ to Val in the calcium binding motif of hPLSCR3 (F258V-hPLSCR3) resulted in slower growth, reduced levels of mitochondrial mass, transmembrane potential, intracellular ATP and mitochondrial respiration (Liu *et al.*, 2003). Alternatively, mutation of $Phe^{281}$ in hPLSCR1 resulted in complete loss of metal binding and scramblase activity (Zhou *et al.*, 1998b). The relative difference in the point mutant of hPLSCR3 and hPLSCR1 could be either by (i) the mutant F258V-hPLSCR3 only diminished but did not abolish the functional activity of the protein or (ii) an alternate mechanism for CL exposure. Since F258V-hPLSCR3 did not show complete loss of activity in cell lines, it is important to know whether hPLSCR3 really does scrambling of phospholipids *in vitro*. If it does, it will be important to study the PL specificity and metal-ion binding. These unknown queries intrigued us to study its biochemical features. In this study, we have purified recombinant wt-hPLSCR3 and a calcium binding mutant, F258V-hPLSCR3 to homogeneity and performed functional and structural studies.

## Functional assay

### Activity

Scramblases are calcium dependent translocators of PLs between the lipid bilayer. In order to measure the functional activity of the protein, assays were performed either with inside or outside labelled proteoliposomes and not with symmetrical labelled, since scramblases accelerate bidirectional scrambling of PLs, the net change in fluorescence becomes negligible in symmetrical labelling. In case of outside labelled vesicles, the NBD-PLs were incorporated in the outer leaflet of the bilayer (Supplementary Figure S1B). Upon dithionite addition (membrane impermeable quencher), NBD-PLs on the outer leaflet of liposomes and proteoliposomes incubated with EDTA were quenched, leading to a decrease in 80% of fluorescence. In case of proteoliposomes with $Ca^{2+}$, the incorporated protein translocates the NBD-PLs from outer to inner leaflet, protecting from dithionite thereby retaining the

fluorescence. Since scramblases translocate bidirectionally, some of the translocated NBD-PLs were flipped back to the outer leaflet to be quenched by dithionite, resulting in further loss of fluorescence. Hence in total ~60-70% of fluorescence is lost (Figure S1D). The fluorescence values after dithionite addition were normalized and the difference in residual fluorescence between $Ca^{2+}$ treated proteoliposomes and that of EDTA treated proteoliposomes were represented as the activity of scramblase.

In case of inside labelled vesicles, ~40 % of NBD-PLs were incorporated in the inner leaflet of the bilayer and the rest were quenched on dithionite addition during reconstitution (Figure S1A). In case of liposomes and proteoliposomes with EDTA dithionite addition results in ~15-20% loss in fluorescence and in case of proteoliposomes with $Ca^{2+}$, the activated scramblase translocates the NBD-PLs from inner leaflet to the outer leaflet resulting in further loss of fluorescence (~25-40%) by dithionite during the assay time. A maximum difference of only 20% loss in fluorescence is observed because the reconstituted scramblase back flipped the translocated NBD-PLs from outer to inner leaflet preventing the quenching (Figure S1C).

Scramblase disrupts the asymmetry of the bilayer by scrambling of PLs between two leaflets of the membrane. No reports have shown that scramblases are involved in promoting equilibrium or symmetry of the PLs in the membrane bilayer. Theoretical expectation of 50% scramblase activity by complete equilibration of NBD-PLs between the bilayer was not achieved. The obtained activity of ~10% is in accordance with previous reports, where recombinant hPLSCR1 showed ~5% to 18% translocation (Zhou *et al.*, 1998, Francis *et al.*, 2012, Shettihalli and Gummadi, 2013) and recombinant hPLSCR4 showed ~10% translocation of phospholipids (Francis and Gummadi, 2012) .Translocation of NBD-PL increased with increasing protein/lipid ratio but never achieves 50% (Bassé *et al.*, 1996). The reduced activity is a reflection of one-third of the protein being reconstituted in to proteoliposomes have inward facing $Ca^{2+}$ binding site, and cannot be activated by external $Ca^{2+}$ and also as a result of back flipping of translocated NBD-PLs. The reduced activity is also a reflection of one-third of the protein being reconstituted in to proteoliposomes have inward facing $Ca^{2+}$ binding site, and cannot be activated by external $Ca^{2+}$.

Mitochondrial outer membrane has 54% PC, 29% PE, 2% PS and 1% CL and the inner membrane has 40% PC, 34% PE, 3% PS and 18% CL (Daum and Vance, 1997). The labelled form of predominant PLs present in mitochondria viz. NBD-PC, NBD-PS, NBD-PG and

NBD-PE were chosen for assaying for scramblase activity. NBD labelled PLs are chosen since the functions of proteins involved in translocation and flip-flop of various lipid species are unperturbed by these exogenously added labelled lipids (Chattopadhyay, 1990). Moreover, NBD as a fluorophore does not interfere with PLs flip-flop and hence been extensively used in translocation studies as a tool to measure scramblase activity (McIntyre and Sleight, 1991, Angeletti and Nichols, 1998, Ploier and Menon, 2016). Spectroscopic studies of various NBD labelled lipids in model and biological membranes from previous studies revealed that these labelled lipids gets incorporated at appropriate positions in the membranes thereby replicating the bilayer (Balch *et al.*, 1994). The translocation studies with NBD-PLs revealed that hPLSCR3 is head-group specific in translocation. Hence, scramblase assay with NBD-PC, NBD-PE, NBD-PS and NBD-PG were performed.

wt-hPLSCR3 specifically translocated PE compared to PS, PC and PG unlike hPLSCR 1 and 4 which showed head group non-specific scramblase activity (Francis and Gummadi, 2012, Francis *et al.*, 2012a, Rayala *et al.*, 2014) and a 50% loss of activity was observed in the mutant F258V-hPLSCR3. Several reports exist on the overlapping functions of PE and CL in the mitochondrial membrane (Joshi *et al.*, 2012, Böttinger *et al.*, 2012). These two non-bilayer forming phospholipids play vital roles in maintaining mitochondrial morphology, membrane potential and fusion. Though cells lacking CL or PE were viable, loss of both the phospholipids is lethal, suggesting that PE and CL could be compensated for each other and are essential to the mitochondrial function(Joshi *et al.*, 2012). The reason for the preference of hPLSCR3 towards PE and CL is not yet certain and should be further investigated.

**Metal-ion binding**

Intrinsic tryptophan fluorescence studies were performed to understand the metal ion binding properties of hPLSCR3. Interestingly, our results revealed that $Ca^{2+}$ exhibited affinity to wt-hPLSCR3 (23.31 mM ± 1.90 mM) similar to that of hPLSCR1 (25.4 ± 2.6 mM), whereas $Mg^{2+}$ (20.98 mM ± 1.55 mM ) exhibited similar affinity as that of $Ca^{2+}$ to wt-hPLSCR3 but higher than that of hPLSCR1 (151.8 mM ± 31.0 mM (Rayala *et al.*, 2014). The results incongruous to our previous study where the calcium binding peptide of wt-hPLSCR3 exhibited significantly more affinity to $Ca^{2+}$ than to $Mg^{2+}$ (Sahu *et al.*, 2009) suggesting a possible $Mg^{2+}$ binding site apart from the $Ca^{2+}$ binding motif. While the peptides could be used as tools to study the biochemical properties of specific motifs, the results might not be consistent with the native proteins. The calcium binding mutant, F258V-hPLSCR3 exhibited

a three-fold reduction in the binding affinity to $Ca^{2+}$ and around four-fold reduction in the binding affinity to $Mg^{2+}$ when compared to wt-hPLSCR3. The calcium binding affinities of wt-hPLSCR3 were similar to hPLSCR1 and slightly higher than that of hPLSCR4 (Sahu *et al.*, 2009, Francis and Gummadi, 2012) thereby implying that the underlying functional mechanism of the three proteins might be similar.

The concentration of $Ca^{2+}$ is 10-100 nM within cells and 2 mM in blood (BNID: 100130, 110746 and 11136) and that of $Mg^{2+}$ is 0.5 mM and 1 mM (BNID: 104983, 100770 and 101953) respectively (Milo *et al.*, 2010). The intracellular $Ca^{2+}$ concentration increases by 1000-fold on certain cellular conditions such as cell injury and apoptosis. An increase in intracellular $Ca^{2+}$ due to cell injury or apoptosis causes rapid bidirectional movement of phospholipids between leaflets in plasma membrane mediated by hPLSCRs (Zhao *et al.*, 1998a). The affinity for $Ca^{2+}$ in the concentration range of mM prominently reveals that the protein is functionally active upon calcium binding at such high concentration as seen in previous reports where recombinant hPLSCR1 sequestered ~10 % NBD-PC in presence of 1-10 mM $Ca^{2+}$ and only ~2-6% of NBD-PC were sequestered in presence of 0.001-0.1 mM $Ca^{2+}$ (Zhou *et al.*, 1998a). Therefore these affinity values obtained *in vitro* suggest that the hPLSCR3 becomes functionally active under cellular conditions like injury and apoptosis, otherwise only basal level of scrambling is observed.

The $Ca^{2+}$ binding motif in hPLSCR3, $^{250}$DADDFGLQFPLD$^{261}$ (IV in Figure 1D) is highly conserved among the scramblase family across species. The novel scramblase-like $Ca^{2+}$ binding motif differs from the classical EF type 2 signature sequence 'D-{W}-[DNS]-{ILVFYW}-[DENSTG]-[DNQGHRK]-{GP)-[LIVMC]-[DENQSTAGC]-x(2)-[DE]-[LIVMFYW]' (PROSITE accession no. PS00018) by the presence of a phenylalanine at position 9. Mutation studies in the $Ca^{2+}$ binding motif of hPLSCR1 revealed that alanine substitution at Asp $^{275}$ and Phe $^{281}$ resulted in 100% loss of scramblase activity *in vitro* (Zhou *et al.*, 1998b). The corresponding amino acid in wt-hPLSCR3, Phe $^{258}$ mutated to Val and over expressed in HEK293 cells resulted in impaired mitochondrial processes. Our results collectively indicate that F258V-hPLSCR3 diminished but not abolished the metal binding ability and scramblase activity. The observed results corroborates with the *in-vivo* studies reported previously. Hence Phe$^{258}$ might play a supporting role in the octahedral co-ordination of $Ca^{2+}$, whereas Asp$^{250}$, Asp$^{252}$, Asp$^{261}$ might be crucial for $Ca^{2+}$ binding. Mutations in the aspartate at position 1, 3 and 12 might directly affect the $Ca^{2+}$ binding to protein which should be investigated.

**Surface hydrophobicity**

Circular dichroism studies revealed that the wt-hPLSCR3 exhibited similar CD signature to hPLSCR1 (Francis *et al.*, 2012a). $Ca^{2+}$ and $Mg^{2+}$ binding did not affect the secondary structure of both wt-hPLSCR3 and F258V-hPLSCR3. $Ca^{2+}$ and $Mg^{2+}$ binding mediated local conformational changes exposing the hydrophobic core was probed by ANS. Both wt-hPSLCR3 and F258V-hPLSCR3 with $Ca^{2+}$ and $Mg^{2+}$ underwent local conformational changes and resulted in an increase of surface hydrophobicity similar to the observations made for hPLSCR1, hPLSCR2 and hPLSCR4 (Francis and Gummadi, 2012, Rayala *et al.*, 2014).

**Aggregation**

Changes in surface hydrophobicity upon metal ion binding might result in protein-protein interactions or oligomerization of the protein (Tyedmers *et al.*, 2010). Both wt-hPLSCR3 and F258V-hPLSCR3 underwent aggregation upon $Ca^{2+}$ and $Mg^{2+}$ binding similar to hPLSCR1 where proline-rich domain (PRD) of hPLSCR1 was responsible for oligomerization mediated scramblase activity (Rayala *et al.*, 2014). Hence, we strongly suggest that WT-hPLSCR3 could also oligomerize in the presence of $Ca^{2+}$ and their functional mechanism might be similar. Studies on the oligomerization of hPLSCR3 could lead to a better understanding of the functional mechanism of the scramblase proteins.

To conclude, this is the first report on $Ca^{2+}$ induced translocation of phospholipids by hPLSCR3. Apart from CL, hPLSCR3 was found to exhibit specificity towards amino phospholipids, PE over other phospholipids unlike hPLSCR1 which did not show any head group preference. Metal ion-induced conformational studies revealed that hPLSCR3 binds weakly to $Ca^{2+}$ that triggers changes to surface hydrophobicity and aggregation which is essential for the functioning of the protein. A functionally inactive mutant F258V-hPLSCR3, showed loss of PL translocation activity, reduced binding affinity to metal ions, but exhibited metal ion induced surface hydrophobicity changes and aggregation. Further studies on the unique specificity of hPLSCR3 for CL, PE and PS, oligomerization, mitochondrial localization, and interaction with other mitochondrial proteins might lead to novel insights on the unique functional characteristics of this protein.

# Materials and methods

## Materials

N-lauryl sarcosine (NLS), egg phosphatidylcholine (egg PC), phosphatidylserine (PS), molecular biology-grade $CaCl_2$ and phenyl methane sulfonyl fluoride (PMSF) were obtained from Sigma (USA); *E. coli* DH5 α and *E. coli* Rosetta (DE3) strains were obtained from ATCC (USA). The cDNA of hPLSCR3 was purchased from plasmid repository DNASU (clone ID: HsCD00045430; Arizona, USA) (Cormier *et al.*, 2010, 2011, Seiler *et al.*, 2014) and pET-28 a(+) was obtained from Novagen (USA). Fluorescent-labelled lipids, 7-nitrobenz-2-oxa-1,3-diazol-4-yl-phosphatidyl choline (NBD-PC), 7-nitrobenz-2-oxa-1,3-diazol-4-yl-phosphatidylserine (NBD-PS), 7-nitrobenz-2-oxa-1,3-diazol-4-yl-phosphatidyl glycerol (NBD-PG) and 7-nitrobenz-2-oxa-1,3-diazol-4-yl-phosphatidylethanolamine (NBD-PE) were purchased from Avanti Polar Lipids, Inc. (USA). SM2 Bio-Beads and protein molecular weight markers were obtained from BioRad, (USA). The $Ni^{2+}$-NTA matrix was purchased from Qiagen (USA). Kanamycin, chloramphenicol, dithiothreitol (DTT), molecular biology grade sodium chloride (NaCl), tris(hydroxymethyl) aminomethane, isopropyl β-D-1-thiogalactopyranoside (IPTG), ethylene diamine tetraacetic acid (EDTA), and other routine chemicals were purchased from Himedia (India).

## Plasmid construction

hPLSCR3 (UNIPROT Accession number: Q9NRY6) ORF was directionally cloned between the NheI and BamHI sites of the pET-28 a(+) expression vector maintaining the reading frame. The ORF was amplified using forward primer 5′-CGG CTA GCC GTA TGG CAG GCT ACT TGC CCC-3 ′ and reverse primer 5′-CGG GAT CCC GCT AAC TGG TGA CGG CAG AGG-3′ containing NdeI and BamHI sites, respectively. PCR-amplified product was then digested with NdeI and BamHI and ligated into pET-28 a(+) vector. The cloned insert was further verified by sequencing. Site-directed mutagenesis was generated using forward primer 5'-TGG CCT ACA GGT CCC GCT GGA CC-3' and reverse primer 5'-CAG CGG GAC CTG TAG GCC AAA GTC ATC-3', and presence of the mutation was confirmed by sequencing.

## Overexpression of the recombinant wt-hPLSCR3 and F258V-hPLSCR3

Transformation of the wt-hPLSCR3-pET-28 a(+) and F258V-hPLSCR3 plasmids into the *E. coli* Rosetta (DE3) strain was performed by heat shock method. The transformants were then selected on an LB agar plate containing 50 μg/ml kanamycin and 35 μg/ml chloramphenicol. A single colony was then inoculated into the LB broth containing 50 μg/ml kanamycin and 35 μg/ml chloramphenicol and was grown at 37°C and 180 rpm until $A_{600}$ reached ~ 0.6-0.8. The cells were then induced with 0.3 mM IPTG, and were maintained at 37°C and 180 rpm for 6 h. Induced cells (1 g) were harvested by centrifugation at 4°C for 5 min at 8500 *g* and resuspended in 10 ml buffer containing 20 mM Tris-HCl (pH 7.4), 200 mM NaCl, 1 mM PMSF, 1 mM EDTA, and 1 mM DTT. The cell suspension was then subjected to ultrasonication for 4 min (4 s on/4 s off) at 30% amplitude. The soluble and insoluble fractions were separated by centrifugation at 4°C for 20 min at 16 000 *g* and the protein expression was analyzed on 12% SDS-PAGE.

## Purification of 6× His tag-wt-hPLSCR3

The insoluble fraction was resuspended in 10 ml of buffer A (20 mM Tris-HCl (pH 7.4), 200 mM NaCl) with 0.3% (v/v) NLS as described earlier (Francis *et al.*, 2012a). The suspension was agitated for 16 h at 110 rpm at 16 °C followed by centrifugation at 16 000 *g* for 15 min at 4°C. Subsequently, in buffer A, NLS was replaced with 0.025% (w/v) Brij-35 (buffer B) in further steps of purification. The supernatant was then subjected to dialysis with 10-kDa cut-off membrane against buffer B, with three buffer changes every 12 h. Absorbance at 215 nm was used to determine the amount of the residual NLS present after dialysis (Burgess, 1996, Francis *et al.*, 2012a). The protein solution was then loaded onto a Ni-NTA column, equilibrated with buffer containing 20 mM Tris-HCl (pH 7.4) and 200 mM NaCl, before use. Binding was carried out for 3 h at 4°C, and the protein was finally eluted out with buffer B containing 250 mM imidazole. The eluted protein was then repeatedly dialyzed against buffer B to completely remove the imidazole. The purification of the F258V mutant of hPLSCR3 was done similarly as described above. The expressed and purified proteins were confirmed by western blotting with anti-PLSCR3 antibody (SC68123, Santacruz, USA).

## Size-exclusion chromatography

The purified protein was subjected to size-exclusion fast protein liquid chromatography (FPLC) using a Superdex-200 column. Total column volume was 120 ml, with a void volume

(Vo) of 35.19 ml. The elution was carried out using buffer B with a flow rate of 0.75 ml/min. Protein standards were used to calibrate the column. From the standard plot, the approximate molecular weight of the purified protein was determined using the elution volumes (Ve).

## Reconstitution of hPLSCR3 into proteoliposomes

hPLSCR3 was reconstituted into outside labelled and inside labelled proteoliposomes containing exogenous PLs (10% PS and 90% PC) at 4.5 μmol of total PLs as previously described (McIntyre and Sleight, 1991, Bassé *et al.*, 1996, Francis and Gummadi, 2012).

### Outside labelling

Briefly, egg PC and PS were dried under $N_2$, then solubilized in 10 mM HEPES/NaOH (hydroxyethyl-1-piperazine ethanesulfonic acid/sodium hydroxide), pH 7.5, 100 mM NaCl, and 1% (w/v) Triton X-100, and 100 μg of wt-hPLSCR3 or F258V-hPLSCR3 were added. The detergent was slowly removed using SM2 Biobeads. Similarly, liposomes were prepared following the same procedure without wt-hPLSCR3 and F258V- hPLSCR3. The liposomes and proteoliposomes were collected by ultracentrifugation using an MLA130 rotor in Optima Max-XP tabletop centrifuge (Beckman Coulter ultracentrifuge, USA) and washed 3 times by centrifuging at 2,30,000 *g* for 30 min with the assay buffer (10 mM HEPES/NaOH, pH 7.5, and 100 mM NaCl). The vesicles were extruded using a 0.1 μm polycarbonate membrane filter to make uniform sized unilamellar vesicles. After extrusion, liposomes and proteoliposomes were labelled with 0.3 mol% of NBD-PLs (Avanti Polar Lipids, USA) to form outside labelled vesicles (Figure S1B).

### Inside labelling

Egg PC, PS and NBD-PLs were dried under $N_2$, then solubilized in 10 mM HEPES/NaOH pH 7.5, 100 mM NaCl, and 1% (w/v) Triton X-100, and 100 μg of wt- hPLSCR3 or F258V-hPLSCR3 were added. The detergent was slowly removed using SM2 Biobeads. Similarly, liposomes were prepared following the same procedure without wt-hPLSCR3 and F258V-hPLSCR3. The liposomes and proteoliposomes were collected by ultracentrifugation and washed 3 times by centrifuging at 2,30,000 *g* for 30 min with the assay buffer (10 mM HEPES/NaOH, pH 7.5, and 100 mM NaCl). The vesicles were extruded using a 0.1 μm polycarbonate membrane filter to make uniform sized unilamellar vesicles. After extrusion, 20 mM sodium dithionite, a membrane impermeable quencher was added to irreversibly

quench the fluorescent lipids in the outer leaflet to create inside labelled vesicles. The inside labelled vesicles were further washed with the assay buffer twice (Supplementary Figure S1A).

## Scramblase assay

Scramblase activity was measured for outside-labelled & inside labelled proteoliposomes (Scheme described in Figure S1). Briefly, proteoliposomes containing NBD-PLs were incubated for 4 h at 37°C in 10 mM HEPES/NaOH (pH 7.5), 100 mM NaCl in the presence of 3 mM $Ca^{2+}$, 3 mM $Mg^{2+}$ or 3 mM EDTA and was transferred to a stirred spectrofluorometer (Perkin Elmer LS-55). Sample fluorescence (excitation 470 nm and emission 532 nm) was monitored continuously at 25 °C with constant low-speed stirring and slit widths of 10 nm (excitation) and 10 nm (emission). Fluorescence was recorded continuously for 600 s in a spectrofluorometer. After 200 s, freshly prepared 20 mM dithionite (in 1 M Tris Base pH-11.6) was added. Fluorescence was monitored for the next 400 s. The difference between the non-quenchable fluorescence observed in the presence of metal ions and EDTA was attributed to the metal ions -induced scrambling of NBD-PLs.

Scramblase activity was calculated as:

Outside labelling: Scramblase activity (% NBD-PL translocated) = $F_{\text{metal-ion}} - F_{\text{EDTA}}$,

Inside labelling: Scramblase activity (% NBD-PL translocated) = $F_{\text{EDTA}} - F_{\text{metal-ion}}$,

where $F_{\text{metal-ion}}$ is the relative fluorescence intensity in the presence of metal ions and $F_{\text{EDTA}}$ is the relative fluorescence intensity in the presence of EDTA.

## Intrinsic tryptophan fluorescence spectroscopy

Fluorescence emission spectra was recorded at wavelengths between 300 and 500 nm, with an excitation wavelength of 295 nm at 25°C at a scanning speed of 100 nm/min, and the band passes were 5 nm each. Metal ion stock solutions (1 M) were freshly prepared and used for titration studies. The cuvettes were rinsed with deionized water before use. The wt-hPLSCR3 and F258V-hPLSCR3 was titrated with small aliquots of respective metal ions, and the binding constants ($K_d$) of metal ions to protein were determined by Scatchard plot using nonlinear curve fitting (Prism 5.0 GraphPad Software Inc.,San Diego, USA).

A graph for fraction of ligand sites occupied $[(F_0 - F)/(F_0 - F_{sat})]$ vs ligand concentration is drawn and curve fitting is done using one site binding non-linear regression analysis, where $F_0$ is the fluorescence in the absence of a ligand, $F_{sat}$ is the fluorescence at saturated ligand concentration, and F is the fluorescence in the presence of a particular ligand concentration.

## Protein surface hydrophobicity changes by ANS fluorescence

ANS-binding measurements were recorded using Perkin Elmer LS-55 spectrophotometer at 25°C. ANS binding to protein was monitored between emission wavelengths of 400 and 600 nm with excitation at 365 nm. Scanning conditions were scan speed of 100 nm/min and a bandwidth of 10 nm each. ANS was added to 2 μM protein such that the final concentration of ANS in solution remained 20 μM. To this ANS-protein complex, small increments of metal ions were added and spectra were recorded.

## Far-UV CD studies

The far-UV CD spectra were recorded using Jasco J-810 spectropolarimeter (Easton, MD, USA) at 25°C with a thermostated cell holder. Buffer and sample spectra were recorded at a wavelength range of 190-250 nm in a 0.1 cm path length cuvette. Scanning was done at a scan speed of 10 nm/min with a bandwidth of 2 nm. Protein concentrations of 10 μM were used for far-UV-CD recordings. Buffer spectra was collected under similar conditions and subtracted from that of samples to obtain the final spectra.

## Aggregation studies

The UV absorbance spectra were recorded using a Jasco V-550 spectrophotometer and monitored for a time period of 1200 s. Absorbance was monitored at a wavelength of 360 nm with a bandwidth of 1 nm. Protein concentration of 2 μM was used and metal ions of increasing concentration were added to monitor the aggregation within 1200 s.

## Sequence analysis

CLUSTAL-Omega (EMBL-EBI) was used for multiple sequence alignment (McWilliam *et al.*, 2013) and Espript 3.0 was used for visualizing conserved regions from the multiple sequence alignment (Robert and Gouet 2014). Adobe Illustrator CC 2015 was used for drawing the Schemes and Figures.

### Statistical analysis

Statistical analysis was performed using One Way ANOVA and Tukey's multiple comparison test $p<0.001$ was considered significant. Also two-tailed unpaired t-test was performed where $p<0.05$ was considered significant.

## Acknowledgements

The authors wish to thank Department of Science and Technology, Government of India and Indian Institute of Technology Madras for Circular Dichroism studies. S.K.P., U.S. and S.M. wish to thank Ministry of Human Resource Development (MHRD), Government of India and Indian Institute of Technology Madras for fellowship.

## Conflict of interest statement

The authors declare no conflicts of financial interest in this study.

## References

Alizadeh-Pasdar, N., and Li-Chan, E.C.Y. (2000). Comparison of protein surface hydrophobicity measured at various pH values using three different fluorescent probes. J. Agric. Food Chem. *48*, 328–334.

Angeletti, C., and Nichols, J.W. (1998). Dithionite quenching rate measurement of the inside-outside membrane bilayer distribution of 7-nitrobenz-2-oxa-1,3-diazol-4-yl-labelled phospholipids. Biochemistry (Mosc.) *37*, 15114–15119.

Balch, C., Morris, R., Brooks, E., and Sleight, R.G. (1994). The use of N-(7-nitrobenz-2-oxa-1,3-diazole-4-yl)-labelled lipids in determining transmembrane lipid distribution. Chem. Phys. Lipids *70*, 205–212.

Bassé, F., Stout, J.G., Sims, P.J., and Wiedmer, T. (1996). Isolation of an erythrocyte membrane protein that mediates $Ca^{2+}$-dependent transbilayer movement of phospholipid. J. Biol. Chem. *271*, 17205–17210.

Bernacchi, S., Mercenne, G., Tournaire, C., Marquet, R., and Paillart, J.-C. (2011). Importance of the proline-rich multimerization domain on the oligomerization and nucleic acid binding properties of HIV-1 Vif. Nucleic Acids Res. *39*, 2404–2415.

Bevers, E.M., Comfurius, P., Dekkers, D.W., Harmsma, M., and Zwaal, R.F.(1998). Transmembrane phospholipid distribution in blood cells: control mechanisms and pathophysiological significance. Biol. Chem. *379*, 973–986.

Böttinger, L., Horvath, S.E., Kleinschroth, T., Hunte, C., Daum, G., Pfanner, N., and Becker, T. (2012). Phosphatidylethanolamine and cardiolipin differentially affect the tability of mitochondrial respiratory chain supercomplexes. J. Mol. Biol. *423*, 677–686.

Burgess, R.R. (1996). Purification of overproduced *Escherichia coli* RNA polymerase sigma factors by solubilizing inclusion bodies and refolding from Sarkosyl. Methods Enzymol. *273*, 145–149.

Cardamone, M., and Puri, N.K. (1992). Spectrofluorimetric assessment of the surface hydrophobicity of proteins. Biochem. J. *282*, 589–593.

Chattopadhyay, A. (1990). Chemistry and biology of N-(7-nitrobenz-2-oxa-1,3-diazol-4-yl)-labelled lipids: fluorescent probes of biological and model membranes. Chem. Phys. Lipids *53*, 1–15.

Cormier, C.Y., Mohr, S.E., Zuo, D., Hu, Y., Rolfs, A., Kramer, J., Taycher, E., Kelley, F., Fiacco, M., Turnbull, G., and LaBaer, J. (2010). Protein Structure Initiative Material Repository: an open shared public resource of structural genomics plasmids for the biological community. Nucleic Acids Res. *38*, D743-D749.

Cormier, C.Y., Park, J.G., Fiacco, M., Steel, J., Hunter, P., Kramer, J., Singla, R., and LaBaer, J. 2011. PSI:Biology-materials repository: a biologist's resource for protein expression plasmids. J. Struct. Funct. Genomics *12*, 55–62.

Daum, G., and Vance, J.E. (1997). Import of lipids into mitochondria. Prog. Lipid Res. *36*, 103–130.

Francis, V.G., and Gummadi, S.N. (2012). Biochemical and functional characterization of human phospholipid scramblase 4 (hPLSCR4). Biol. Chem. *393*, 1173-1181.

Francis, V.G., Majeed, M.A., and Gummadi, S.N. (2012). Recovery of functionally active recombinant human phospholipid scramblase 1 from inclusion bodies using N-lauroyl sarcosine. J. Ind. Microbiol. Biotechnol. *39*, 1041–1048.

Francis, V.G., Mohammed, A.M., Aradhyam, G.K., and Gummadi, S.N. (2013). The single C-terminal helix of human phospholipid scramblase 1 is required for membrane insertion and scrambling activity. FEBS J. *280*, 2855–2869.

He, Y., Liu, J., Grossman, D., Durrant, D., Sweatman, T., Lothstein, L., Epand, R.F., Epand, R.M., and Lee, R.M. (2007). Phosphorylation of mitochondrial phospholipid scramblase 3 by protein kinase C-δ induces its activation and facilitates mitochondrial targeting of tBid. J. Cell. Biochem. *101*, 1210–1221.

Jain, R.K., Chang, W.T., Geetha, C., Joyce, P.B.M., and Gorr, S.-U. (2002). In vitro aggregation of the regulated secretory protein chromogranin A. Biochem. J. *368*, 605–610.

Joshi, A.S., Thompson, M.N., Fei, N., Hüttemann, M., and Greenberg, M.L. (2012). Cardiolipin and mitochondrial phosphatidylethanolamine have overlapping functions in mitochondrial fusion in *Saccharomyces cerevisiae*. J. Biol. Chem. *287*, 17589–17597.

Liu, J., Dai, Q., Chen, J., Durrant, D., Freeman, A., Liu, T., Grossman, D., and Lee, R.M. (2003). Phospholipid scramblase 3 controls mitochondrial structure, function, and apoptotic response. Mol. Cancer Res. *1*, 892–902.

Liu, J., Epand, R.F., Durrant, D., Grossman, D., Chi, N., Epand, R.M., and Lee, R.M. (2008). role of phospholipid scramblase 3 in the regulation of tumor necrosis factor-α-induced apoptosis. Biochemistry (Mosc.) *47*, 4518–4529.

Lott, K., Bhardwaj, A., Sims, P.J., and Cingolani, G. (2011). A Minimal Nuclear Localization Signal (NLS) in human phospholipid scramblase 4 that binds only the minor NLS-binding site of importin α1. J. Biol. Chem. *286*, 28160–28169.

McIntyre, J.C., and Sleight, R.G. (1991). Fluorescence assay for phospholipid membrane asymmetry. Biochemistry (Mosc.) *30*, 11819–11827.

McWilliam, H., Li, W., Uludag, M., Squizzato, S., Park, Y.M., Buso, N., Cowley, A.P., and Lopez, R. (2013). Analysis tool web services from the EMBL-EBI. Nucleic Acids Res. *41*, W597–W600.

Milo, R., Jorgensen, P., Moran, U., Weber, G., and Springer, M. (2010). BioNumbers—the database of key numbers in molecular and cell biology. Nucleic Acids Res. *38* (Suppl. 1), D750–D753.

Pinton, P., Giorgi, C., Siviero, R., Zecchini, E., and Rizzuto, R. (2008). Calcium and apoptosis: ER-mitochondria $Ca^{2+}$ transfer in the control of apoptosis. Oncogene *27*, 6407–6418.

Ploier, B., and Menon, A.K. (2016). A fluorescence-based assay of phospholipid scramblase activity. J. Vis. Exp. *115*, doi: 10.3791/54635.

Posada, I.M.D., Fantini, J., Contreras, F.X., Barrantes, F., Alonso, A., and Goñi, F.M. 2014. A cholesterol recognition motif in human phospholipid scramblase 1. Biophys. J. *107*, 1383–1392.

Rayala, S., Francis, V.G., Sivagnanam, U., and Gummadi, S.N. (2014). N-terminal proline-rich domain is required for scrambling activity of human phospholipid scramblases. J. Biol. Chem. *289*, 13206–13218.

Robert, X., and Gouet, P. (2014). Deciphering key features in protein structures with the new ENDscript server. Nucleic Acids Res. *42*, W320–W324.

Sahu, S.K., Aradhyam, G.K., and Gummadi, S.N. (2009). Calcium binding studies of peptides of human phospholipid scramblases 1 to 4 suggest that scramblases are new class of calcium binding proteins in the cell. Biochim. Biophys. Acta *1790*, 1274–1281.

Sahu, S.K., Gummadi, S.N., Manoj, N., and Aradhyam, G.K. (2007). Phospholipid scramblases: an overview. Arch. Biochem. Biophys. *462*, 103–114.

Shettihalli, A.K., and Gummadi, S.N. (2013). Biochemical evidence for lead and mercury induced transbilayer movement of phospholipids mediated by human phospholipid scramblase 1. Chem. Res. Toxicol. *26*, 918–925.

Sivagnanam,U., Palanirajan, S.K., and Gummadi, S.N. (2017). The role of human phospholipid scramblases in apoptosis: an overview. Biochim Biophys Acta Mol. Cell Res. *1864*, 2261–2271.

Seiler, C.Y., Park, J.G., Sharma, A., Hunter, P., Surapaneni, P., Sedillo, C., Field, J., Algar, R., Price, A., Steel, J., Throop, A., Fiacco, M., and LaBaer, J. (2014). DNASU plasmid and PSI:Biology-Materials repositories: resources to accelerate biological research. Nucleic Acids Res. *42*, D1253-1260.

Tyedmers, J., Mogk, A., and Bukau, B. (2010). Cellular strategies for controlling protein aggregation. Nat. Rev. Mol. Cell Biol. *11*, 777–788.

Van, Q., Liu, J., Lu, B., Feingold, K.R., Shi, Y., Lee, R.M., and Hatch, G.M. (2007). Phospholipid scramblase-3 regulates cardiolipin *de novo* biosynthesis and its resynthesis in growing HeLa cells. Biochem. J. *401*, 103–109.

Wiedmer, T., Zhou, Q., Kwoh, D.Y., and Sims, P.J. (2000). Identification of three new members of the phospholipid scramblase gene family. Biochim. Biophys. Acta *1467*, 244–253.

Zhao, J., Zhou, Q., Wiedmer, T., and Sims, P.J. (1998). Level of expression of phospholipid scramblase regulates induced movement of phosphatidylserine to the cell surface. J. Biol. Chem. *273*, 6603–6606.

Zhao, J., Zhou, Q., Wiedmer, T., and Sims, P.J. (1998). Palmitoylation of phospholipid scramblase is required for normal function in promoting $Ca^{2+}$-activated transbilayer movement of membrane phospholipids. Biochemistry (Mosc.) *37*, 6361–6366..

Zhou, Q., Ben-Efraim, I., Bigcas, J.-L., Junqueira, D., Wiedmer, T., and Sims, P.J. (2005). phospholipid scramblase 1 binds to the promoter region of the inositol 1,4,5-triphosphate receptor type 1 gene to enhance Its expression. J. Biol. Chem. *280*, 35062–35068.

Zhou, Q., Sims, P.J., and Wiedmer, T. (1998). Identity of a conserved motif in phospholipid scramblase that is required for $Ca^{2+}$-accelerated transbilayer movement of membrane phospholipids. Biochemistry (Mosc.) *37*, 2356–2360.

## Figure legends

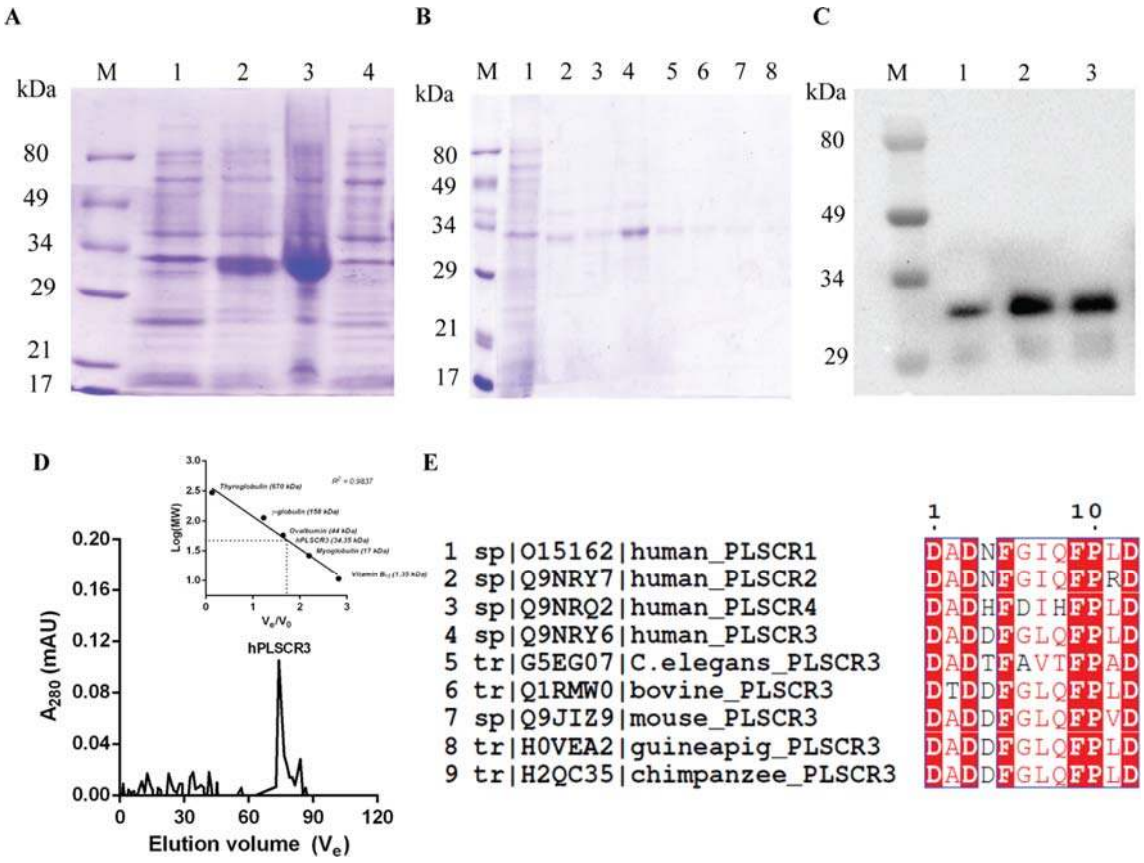


**Figure 1** Overexpression and purification of WT-hPLSCR3.

(A) Cell lysates analysed by 12% SDS PAGE revealing the distribution of expressed protein in inclusion bodies (IBs). Lane M: Marker, lane 1: uninduced cell lysate, lane 2: induced cell lysate, lane 3: insoluble fraction (after NLS treatment), lane 4: soluble fraction (after NLS treatment). (B) Ni-NTA purification of 6× His Tag wt-hPLSCR3. Lane M: Marker, lane 1: soluble fraction (after NLS treatment), lanes 2-7: purified wt-hPLSCR3 (elution with 250 mM imidazole from Ni-NTA column). (C) Western Blot analysis of the cell lysate and the purified fractions of WT-hPLSCR3. Lane M: Marker, lane 1: induced cell lysate WT-hPLSCR3, lane 2: soluble fraction (after NLS treatment), lane 3: purified WT-hPLSCR3. (D) Molecular size determination of purified wt-hPLSCR3 by size-exclusion chromatography. Purified wt-hPLSCR3 [elution volume/void volume (Ve/Vo = 1.8)] corresponds to the monomeric state of the protein (34.3 kDa). (E) Multiple sequence alignment of hPLSCR homologs. Multiple sequence alignment was performed with CLUSTAL-Omega (EMBL-EBI) for the hPLSCR proteins (from top to bottom) are from *Homo sapiens* PLSCR1 (O15162), PLSCR2 (Q9NRY7), PLSCR4 (Q9NRQ2), PLSCR3 (Q9NRY6), *Caenorhabditis elegans* PLSCR3

(G5EG07), *Bos taurus* PLSCR3 (Q1RMW0), *Mus musculus* PLSCR3 (Q9JIZ9), *Cavia porcellus* PLSCR3 (HOVEA2), *Pan troglodytes* PLSCR3 (H2QC35), Espript 3 was used for artwork of the sequence alignment.

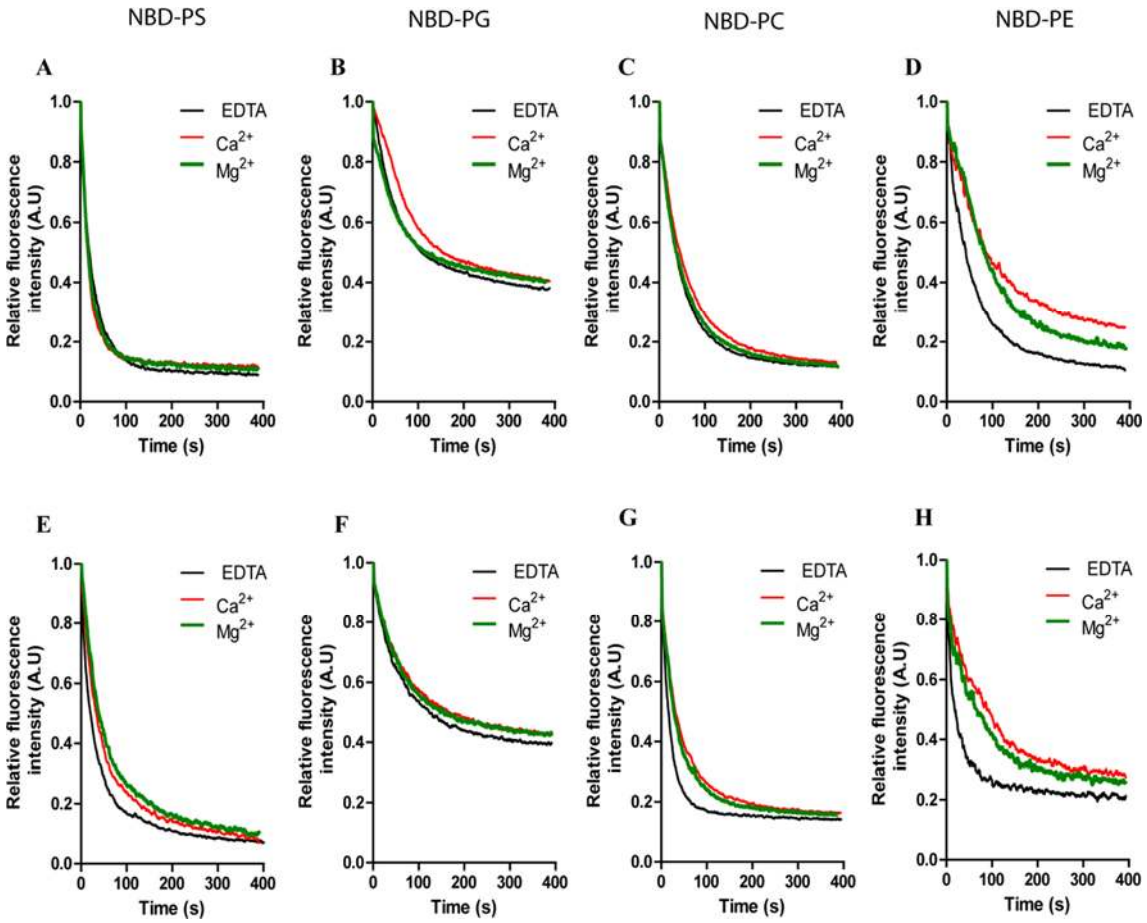


**Figure 2** Scramblase assay. Representative plots for scramblase activity using outside labelled proteoliposomes with WT-hPLSCR3 (A-D) and F258V-hPLSCR3 (E-H).

The scramblase activity is measured by the fluorescence of labelled lipids and the plots represent the loss of fluorescence after dithionite (quencher) addition against time. (A) and (E): NBD-PS labelled; (B) and (F): NBD-PG labelled; (C) and (G): NBD-PC labelled; (D) and (H): NBD-PE labelled. WT shows strong scrambling activity in presence of $Ca^{2+}$ than $Mg^{2+}$. The scrambling activity is reduced in case of calcium binding site mutant in presence of both $Ca^{2+}$ and $Mg^{2+}$. Experiments were repeated in triplicates.

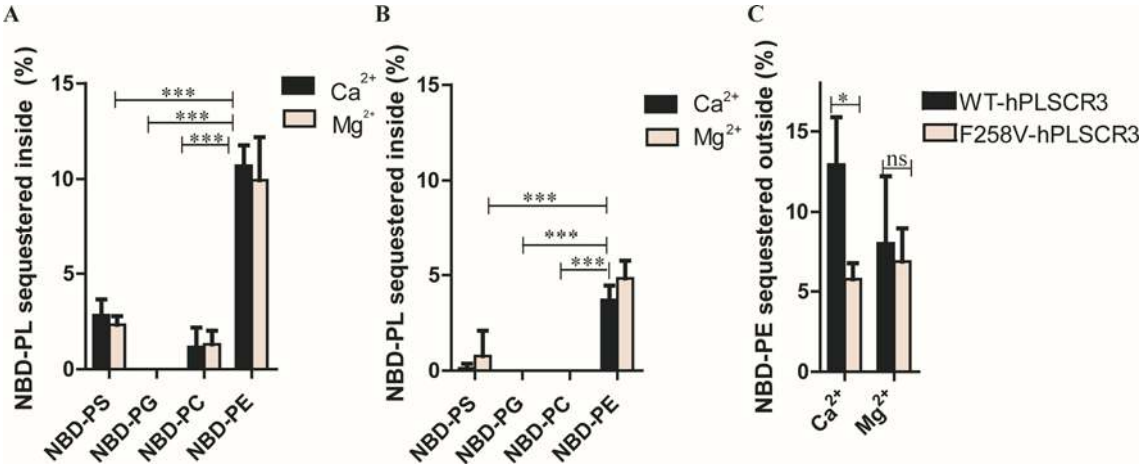


**Figure 3** Scramblase activity as a measure of NBD-PL sequestered.

(A) Scramblase activity using proteoliposomes reconstituted with wt-hPLSCR3. Bar graphs representing the percentage of respective NBD-PLs sequestered inside from outer leaflet. (B) Scramblase activity using proteoliposomes reconstituted with F258V-hPLSCR3. Bar graphs representing the % of respective NBD-PLs sequestered inside from outer leaflet. Results are representative of three independent experiments. Statistical analysis was carried out by one-way ANOVA followed by Tukey's comparison test. ***$p<0.0001$ which is statistically significant. (C) Scramblase activity of wt-hPLSCR3 represented as percentage of NBD-PE sequestered outside from inner leaflet compared against F258V-hPLSCR3 in presence of $Ca^{2+}$ and $Mg^{2+}$. Statistical analysis was performed by two-tailed unpaired t-test. *$p<0.05$ which is significant and ns is non-significant. Proteoliposomes labelled with NBD-PLs were incubated independently with 3 mM EDTA, 3 mM $Ca^{2+}$ and 3 mM $Mg^{2+}$ at 37°C. Among the labelled lipids, NBD-PC, NBD-PS, NBD-PE were translocated by wt-hPLSCR3 and NBD-PS and NBD-PE by F258V-hPLSCR3. NBD-PE is specifically translocated by wt-hPLSCR3 and F258V-hPLSCR3.

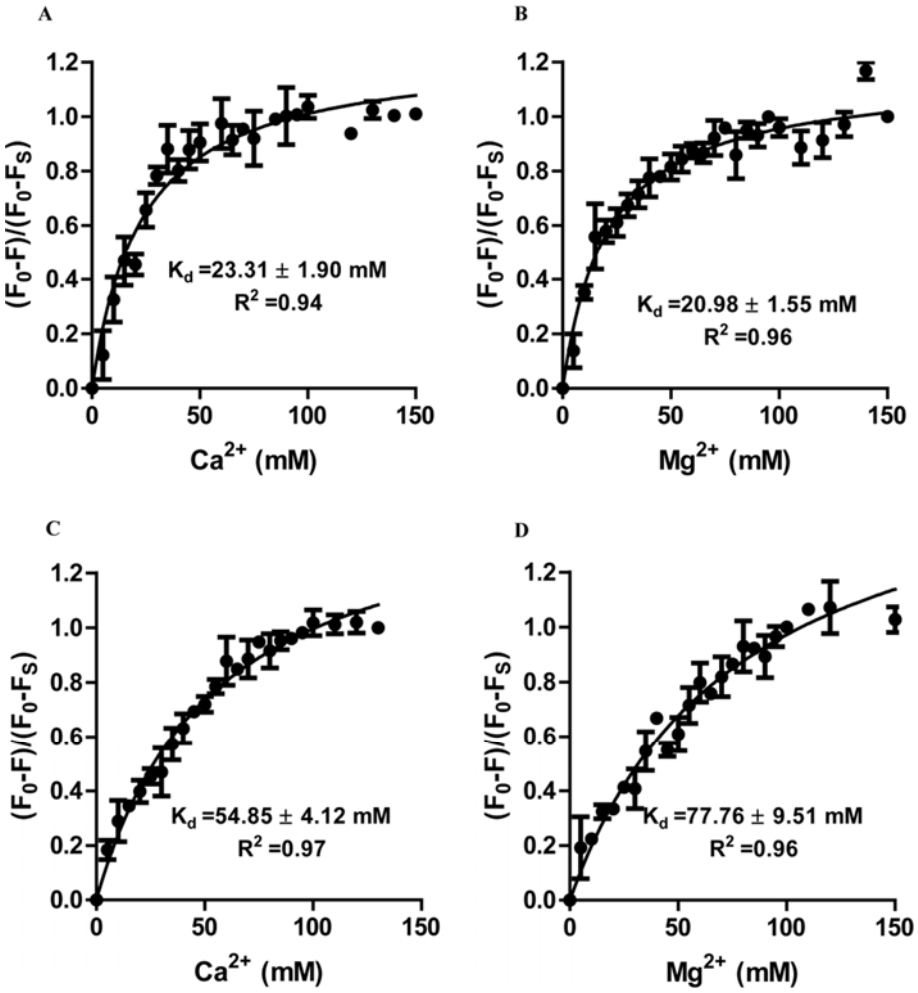


**Figure 4** Intrinsic tryptophan fluorescence.

(A) Scatchard plot for $Ca^{2+}$ binding to wt-hPLSCR3. (B) Scatchard plot for $Mg^{2+}$ binding to wt-hPLSCR3. (C) Scatchard plot for $Ca^{2+}$ binding to F258V-hPLSCR3. (D) Scatchard plot for $Mg^{2+}$ binding to F258V-hPLSCR3. $Mg^{2+}$ ($K_d$=20.98 mM) has higher binding affinity than $Ca^{2+}$ ($K_d$ =23.31 mM) with wt-hPLSCR3. The point mutant has ~three fold lesser affinity for $Ca^{2+}$ ($K_d$=54.85 mM) and ~4 fold lesser affinity for $Mg^{2+}$ ($K_d$=77.76 mM). Results represented here are representative of three independent experiments and error bars represent standard deviation.

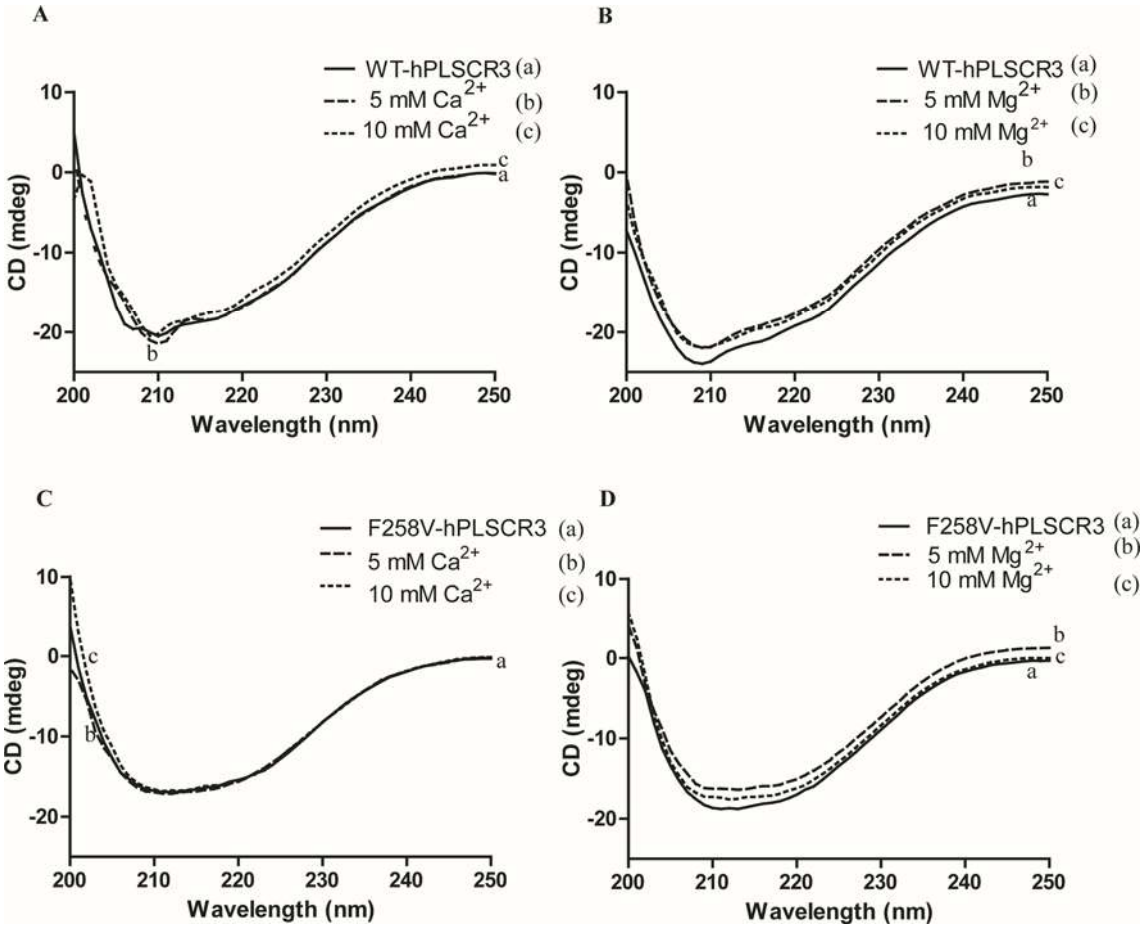


**Figure 5** Far-UV CD Spectra of wt-hPLSCR3 and F258V-hPLSCR3.

(A) Far-UV-CD of wt-hPLSCR3 (apo form) and in the presence of 5 mM and 10 mM $Ca^{2+}$. (B) Far-UV-CD of wt-hPLSCR3 (apo form) and in the presence of 5 mM and 10 mM $Mg^{2+}$. (C) Far-UV-CD of F258V-hPLSCR3 (apo form) and in the presence of 5 mM and 10 mM $Mg^{2+}$. (D) Far-UV-CD of F258V-hPLSCR3 (apo form) and in the presence of 5 mM and 10 mM $Mg^{2+}$. The point mutation has resulted in a structural transition from α-helix to β-sheet. The secondary structure transformation in case of metal ion bound wt-hPLSCR3 and F258V-hPLSCR3 is negligible. Results represented here are representative of three independent experiments.

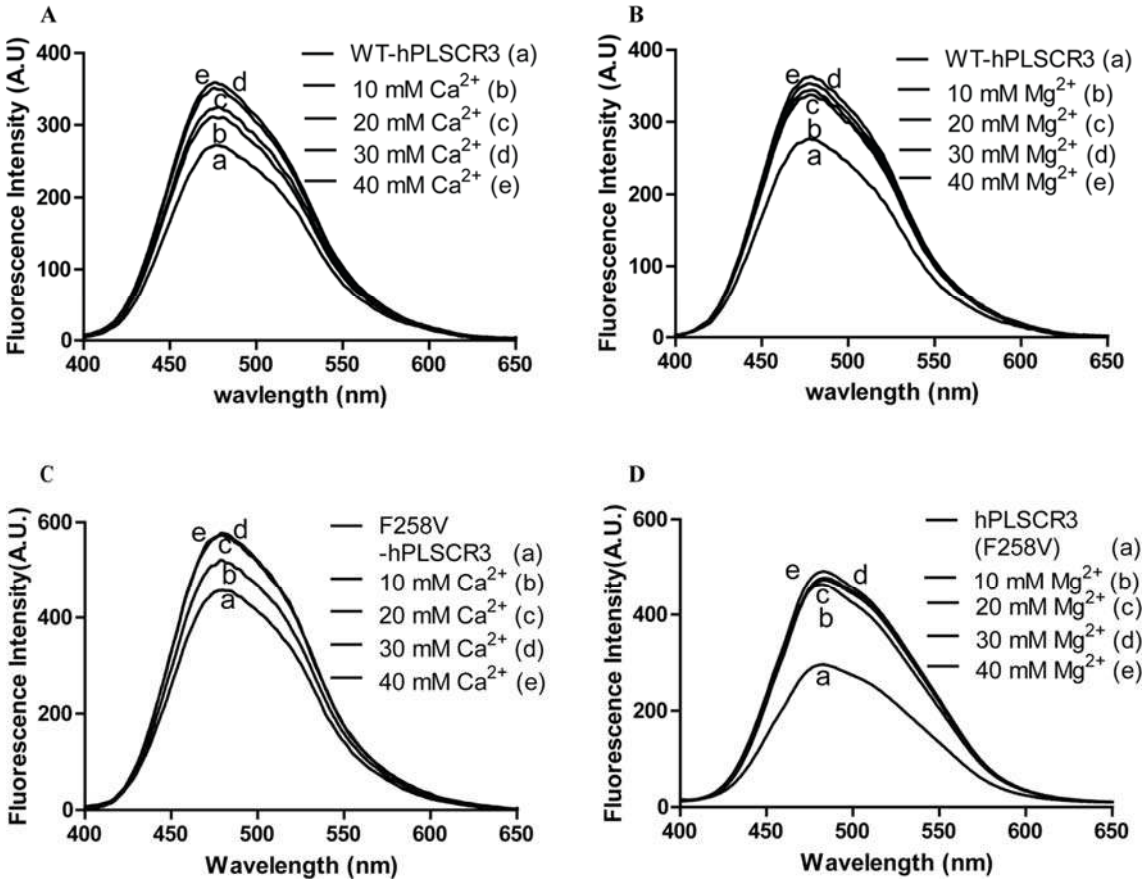


**Figure 6** ANS emission spectra for wt-hPLSCR3 and F258V-hPLSCR3.

(A) ANS binding of wt-hPLSCR3 (apo form) and in the presence of 10 mM, 20 mM, 30 mM and 40 mM $Ca^{2+}$. (B) ANS binding of wt-hPLSCR3 (apo form) and in the presence of 10 mM, 20 mM, 30 mM and 40 mM $Mg^{2+}$. (C) ANS binding of F258V-hPLSCR3 (apo form) and in the presence of 10 mM, 20 mM, 30 mM and 40 mM $Ca^{2+}$. (D) ANS binding of F258V-hPLSCR3 (apo form) and in the presence of 10 mM, 20 mM, 30 mM and 40 mM $Mg^{2+}$. Apoprotein upon metal binding resulted in a local conformational change exposing the hydrophobic patches; as a result, the fluorescence intensity of protein bound ANS dye is increasing. Both wt-hPLSCR3 and F258V-hPLSCR3 underwent a local conformational change upon binding to $Ca^{2+}$ and $Mg^{2+}$, thereby resulting in increase in fluorescence intensity. Results represented here are representative of three independent experiments.

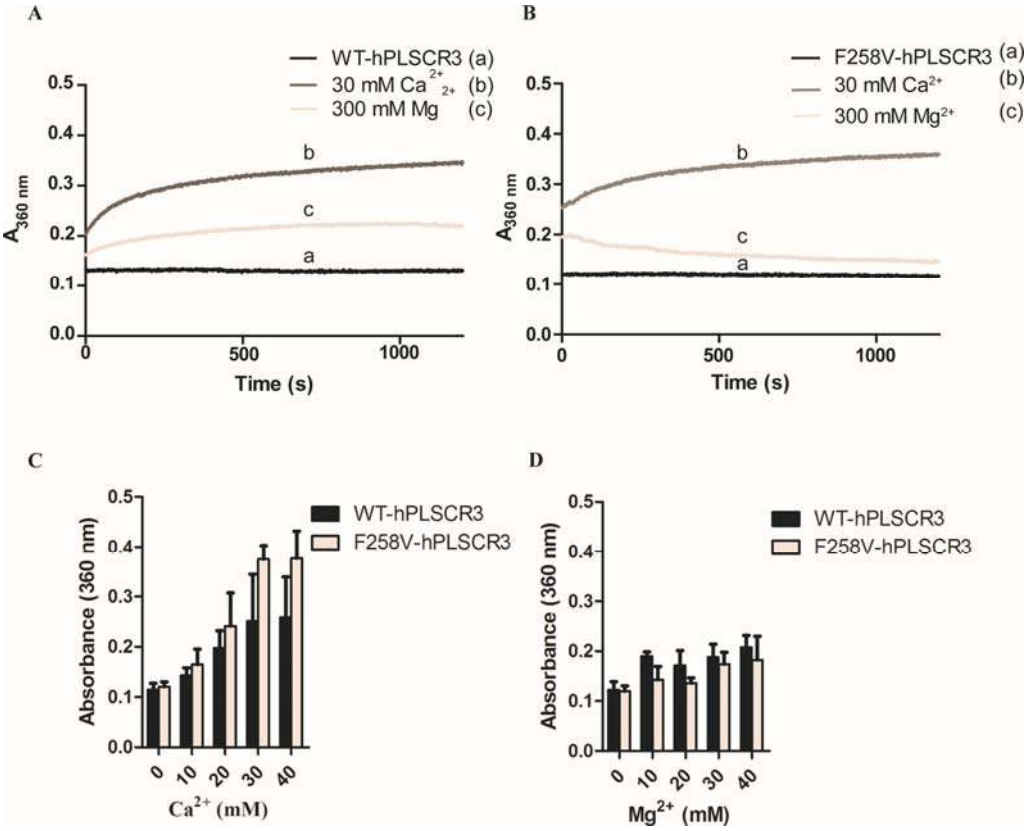


**Figure 7** Aggregation studies for wt-hPLSCR3 and F258V-hPLSCR3.

(A) Aggregation of wt-hPLSCR3. Trace (a) represents wt-hPLSCR3, trace (b) represents aggregation of wt-hPLSCR3 in presence of 30 mM $Ca^{2+}$ and trace (c) represents aggregation of wt-hPLSCR3 in presence of 300 mM $Mg^{2+}$. (B) Aggregation of F258V-hPLSCR3. Trace (a) represents F258V-hPLSCR3, trace (b) represents aggregation of F258V-hPLSCR3 in the presence of 30 mM $Ca^{2+}$ and trace (c) represents aggregation of F258V-hPLSCR3 in the presence of 300 mM $Mg^{2+}$. (C) Aggregation of wt-hPLSCR3 and F258V-hPLSCR3 in the presence of $Ca^{2+}$ represented as increase in the absorbance value measured at 360 nm for different concentrations of the metal ions after 1200 s. (D) Aggregation of wt-hPLSCR3 and F258V-hPLSCR3 in the presence of $Mg^{2+}$ represented as increase in the absorbance value measured at 360 nm for different concentrations of the metal ions after 1200 s. Both wt-hPLSCR3 and F258V-hPLSCR3 oligomerizes on $Ca^{2+}$ binding, whereas the oligomerization rate is less in case of $Mg^{2+}$ bound wt-hPLSCR3 and no aggregation with that of F258V-hPLSCR3. Results represented here are representative of three independent experiments. Statistical analysis was performed by Two-tailed unpaired *t*-test and $p<0.05$ is considered significant. Results indicate that change in aggregation between wt-hPLSCR3 and F258V – hPLSCR3 were not significant in presence of both $Ca^{2+}$ and $Mg^{2+}$.

## Supplementary material

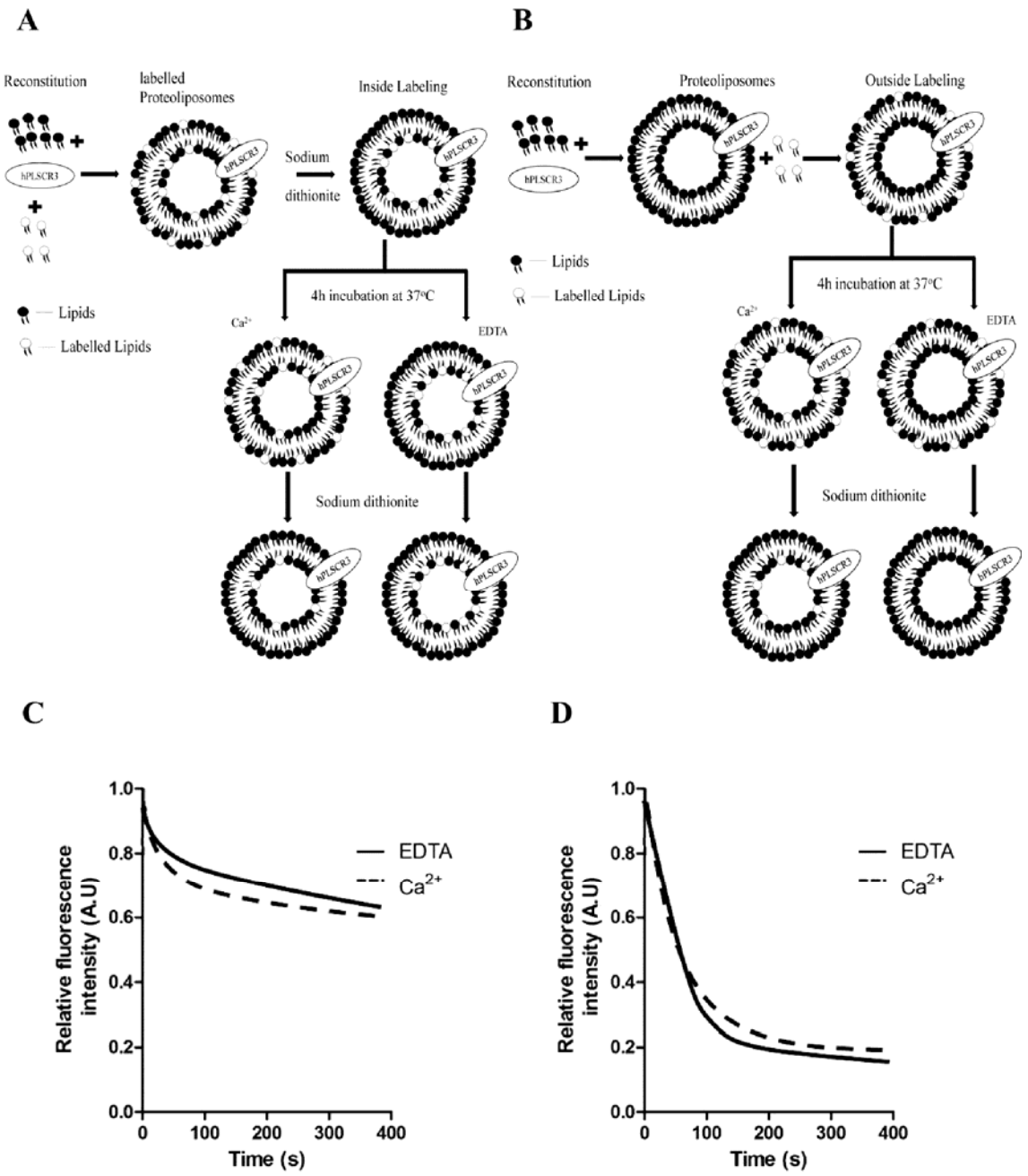


**Figure S1** Schematic representation of the *in vitro* scrambling assay.

(A) Schematic showing the basic steps involved in reconstitution and scramblase assay with labelling in inner leaflet. (B) Schematic showing reconstitution and scramblase assay outer leaflet labelling. Sodium dithionite induced loss of fluorescence of NBD-conjugated lipids in the outer leaflet of artificial liposomes due to bleaching of the fluorophore is monitored with time. (C) & (D) Scrambling of NBD-PL. Representative traces of proteo-liposomes in the presence or absence of $Ca^{2+}$.